Computational flow visualization of shock wave motions

Zonglin Jiang[a] and Kazuyoshi Takayama[b]

[a] LHD, Institute of Mechanics, Chinese Academy Sciences, Beijing 100080, China
[b] SWRC, Institute of Fluid Science, Tohoku University, 2-1-1 Katahira, Aoba-ku, Sendai 980, Japan

ABSTRACT

In this paper, the recent work on computational flow visualization is reported, which is done by simulating optical flow visualization based on the principle that as light passes through flowfields, its phase and direction are changed due to variations of the refractive index induced by non-uniform density in the flow field. Numerical schlieren and interferogram are constructed for three cases. The research shows that these results can be used to assist high-speed photography in visualizing shock wave phenomena more clearly and validating numerical results more reliably.

Keywords: Computational flow visualization, CFD validation, shock wave motion

1. INTRODUCTION

High-speed photography is one of the most valuable tools for the study on shock wave motions. Shadowgraph and schlieren photography, using both monochromatic and colour systems, is widely applied in shock wave research, and interferometry also becomes quite popular in the recent years due to the availability of high-speed pulsed lasers[1-2]. However, the complexity of shock wave motions of interests weakens our ability to highlight shock wave phenomena only by making use of experimental images obtained with high-speed photography because of three-dimensional effects and background noise in test flows. This paper reports our recent work on computational flow visualization, which is done by simulating the high-speed photography, such as schlieren and interferometry. These flow visualizations are based on the common principle that as light passes through a flow field its phase and direction are changed due to variations of the refractive index induced by non-uniform density in shocked flowfields. This makes it possible to analyze physical phenomena that manifest themselves as density changes in the flow field[3-5]. Based on the relation between the refractive index of the light and density variations in the flow field, computational schlieren and interferogram are constructed for three test cases. The research shows that these computational results can be used to assist high-speed photography in the study on shock wave phenomena in complex flow fields. First, the computational flow visualization results can visualize shock wave motions more clearly and can be interpreted more easily. Then, these results also can be compared directly with experiments so that the numerical solutions obtained with computational flow dynamics could be well validated even three-dimensional effects exist in the flowfields under flow visualization. Finally, these three cases will be presented in the following sections to show the feasibility of the computational flow visualization by simulating experimental flow visualization. Computational results will be briefly introduced and interpreted, respectively.

2. PRINCIPLE OF FLOW VISUALIZATION

Interferometry, schlieren and shadowgraph are three techniques widely used in optical flow visualization. These optical techniques use the same principle that as light passes through a flowfield its phase and direction are changed due to variations of the refractive index induced by non-uniform density in the flowfield. Discussions on the above techniques appear in numerous textbooks and in the literature. A brief summary is given here for completeness. In the case of ideal and non-reacting gases, the refractive index n is related to density ρ by the Gladstone-Dale equation.

$$n(x, y, z) = 1 + K_g \rho (x, y, z), \tag{1}$$

where K_g is the Gladstone-Dale constant that changes depending upon gas species and varies slightly with the light wavelength. In holographic interferometry, exposing the film to the object and the reference beam generates double exposure interferogram. For infinite fringe interferometry, as the object beam passes through flowfields, its phase changes due to variations of the refractive index caused by density changes between exposures, but the reference beam does not. The phase shift of the object beam relative to the reference beam between exposures is calculated by integrating

$$\Delta\phi(x_{im}, y_{im}) = \frac{2\pi}{\lambda} K_g \int_0^{Lo} (\rho(x, y, z) - \rho_o)\, dl \tag{2}$$

24th International Congress on High-Speed Photography and Photonics, Kazuyoshi Takayama, Tsutomo Saito, Harald Kleine, Eugene Timofeev, Editors, Proceedings of SPIE Vol. 4183 (2001)

where λ is the wavelength of the light, ρ_o the refractive index of the undisturbed flow and L_o the length of light path through the test section. The image intensity of the infinite-fringe interferogram, I can be calculated by

$$I = 1 + \cos(\Delta\phi(x_{im}, y_{im}) + \phi_o), \tag{3}$$

where (x_{im}, y_{im}) denotes the image plane and ϕ_o is an initial phase shift to compensate for any phase shift between two exposures and is taken as zero in most of the cases. The fringe shift N is given by

This corresponds to the fringe number in infinite-fringe interferogram. Integrating density along the actual light path as the light deflects through the flow field in the test section should be carried out using Eq (2). In the case of finite-fringe

$$N = \frac{1}{2\pi}\Delta\phi(x_{im}, y_{im}) \tag{4}$$

interferogram achieved by tilting the reference beam between exposures, the image intensity is given by

$$I = 1 + \cos(\Delta\phi(x_{im}, y_{im}) + 2\pi v_x x_{im} + 2\pi v_y y_{im}) \tag{5}$$

where v_x and v_y are the special frequency components of the unperturbed fringes.

Schlieren method is also a very popular flow visualization technique. The intensity of each point in schlieren photographs is proportional to the density gradient perpendicular to the knife-edge because the ray deflection is proportional to the density gradient. When the knife is set to be perpendicular to the x-axis in the physical space, the intensity, I is proportional to the integration of the density gradient along the ray.

$$I \propto \int_o^{Lo} \frac{\partial\rho(x,y,z)}{\partial l} dl \tag{6}$$

Shadowgrams are also widely used in aerodynamic experiments. For these, the image intensity is proportional to the gradient of the integration in the direction perpendicular to the light ray, which can be calculated by

$$I \propto grad \int_o^{Lo} grad \quad \rho(x,y,z) dl \tag{7}$$

3. NUMERICAL RESULTS

The three test cases are conducted in the present work aiming at two goals. The first goal is to show the ability of computational flow visualization in visualizing complex shock wave phenomena more clearly and effectively. The other one is to show the possibility of applying the computational flow visualization in validating numerical solutions of computational flow dynamics. The first two cases are designed to approach the first goal and the third case with experimental results is used to demonstrate the validation of numerical simulations.

3.1. Supersonic projectiles discharging from shock tubes

The first test case is a supersonic projectile moving out from a shock tube into open space and the relevant computational results obtained with schlieren method are shown in **Figure 1**. The Mach number of the supersonic projectile is taken as 4.0. Assuming that viscosity effects are negligible in the present shock wave motion at its early stage, this case is computed by solving the Euler equations with a dispersion-controlled scheme. Other two cases are also calculated with the same numerical code and numerical results are processed in form of schlieren or interferogram.

When a supersonic projectile moves within a shock tube, acting as a piston, the precursor shock wave is driven out ahead of the supersonic projectile. The precursor shock wave will discharge from the open-end of the shock tube first, which leads to shock wave diffraction with an associated starting vortex and a jet flow near the open-end. Then, the supersonic projectile moves out of the shock tube, and interacts with this diffracting shock system and the jet flow, as shown in **Figure 1a** and **1b**. Meantime, the high-pressure gas behind the supersonic projectile expands out of the shock tube and the second blast is generated later, as shown in **Figure 1c** and **1d**. The jet flow of the second blast can overtake the supersonic projectile when the pressure behind the projectile is high enough, and will be overtaken again later by the projectile, as shown in **Figure 1e and 1f**. This topic is similar to a gun-firing muzzle blast, usually termed the transitional or intermediate ballistic regime. From **Figure 1**, shock wave interaction, shear layer instability and jet flows can be observed very clearly.

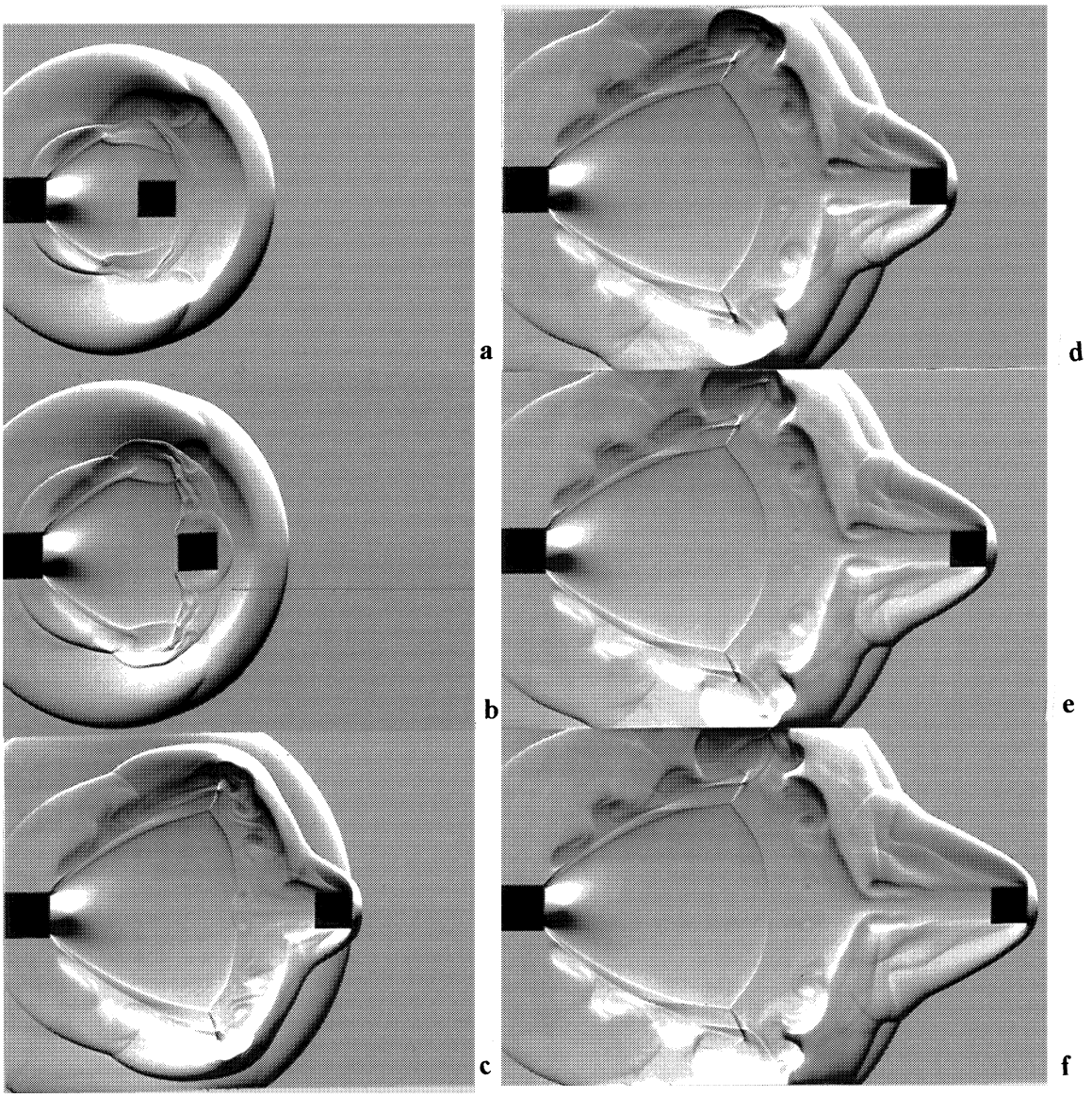

Figure 1. Time sequential schlieren images of shock wave motions created by a supersonic projectile discharging from a shock tube into open space and the Mach number of the supersonic projectile is taken as 4.0.

3.2. Supersonic projectiles moving into a chamber

The test second case is a projectile moving out from a small diameter shock tube into a large chamber and is similar to the first case but that large chamber will create shock wave reflection, which will lead to more complicated shock wave interactions. Time sequential schlieren images of numerical results of case 2 are shown in **Figure 2**. From **Figure 2a**, the precursor shock wave is reflected from the rigid wall of the large chamber and Mach reflection is generated and a jet develops in the vicinity of the 90-degree bend. Once the supersonic projectile moves out of the supersonic flow region bounded by a barrel shock wave and a Mach disc, a bow shock wave is generated in front of the supersonic projectile, as shown in **Figure 2b**. This bow shock can catch up to the precursor shock wave, and will also interact with the reflected shock wave, as shown in **Figure 2c**. Compared with results of case 1, more complicated shock wave flows are developed in this case. However, time sequential schlieren images have visualized the flows very well, and therefore, the ability of computational flow visualization in visualizing complex shock wave phenomena is well demonstrated.

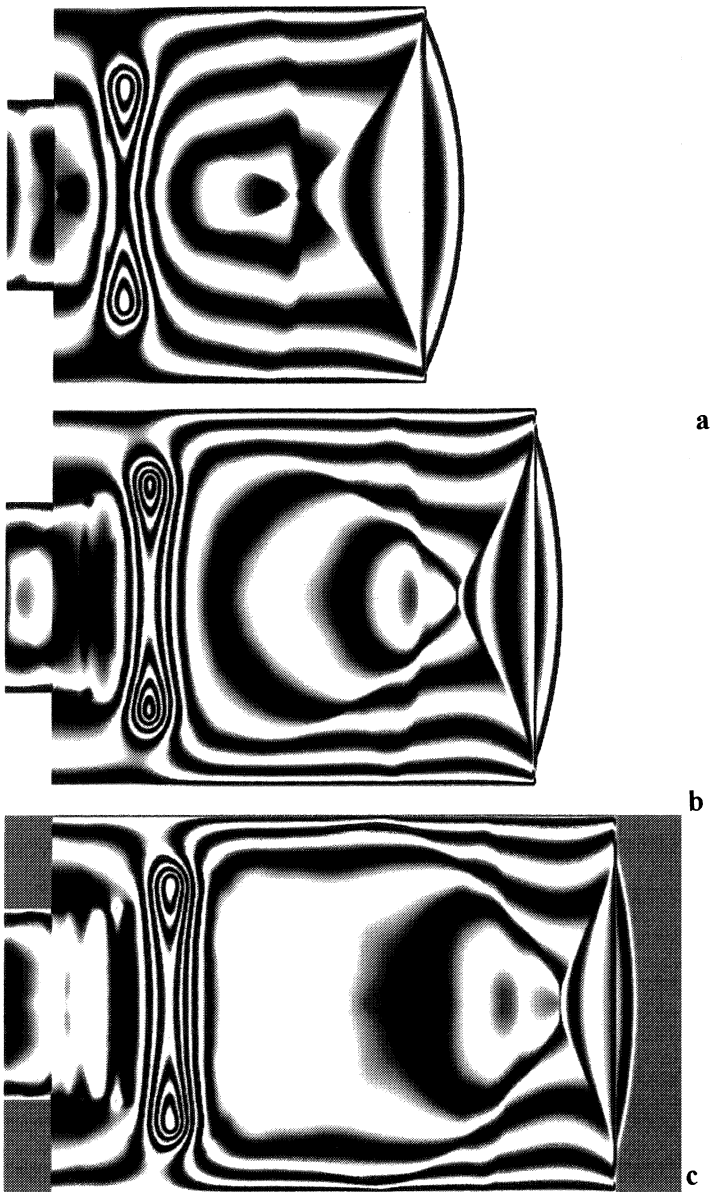

Figure 2. Time sequential schlieren images of shock wave flow driven by a supersonic projectile discharging from a shock tube into a larger chamber and the Mach number of the supersonic projectile is taken as 2.0.

3.3. CFD validations of shock wave motions

Computation flow visualization is not only used to visualize shock wave motions, but also used to validate CFD solutions. The last test cast is designed for this purpose. For the case, shock wave propagation in a tube with sudden area change in its cross section is computed by using the same numerical code as that used for case 1 and 2. The Mach number is taken to be 1.3 and the diameter ratio, the large chamber to the shock tube, is taken as 2:1. This large chamber is specially designed to have an aspheric cross section, which allows the collimated incident ray to traverse the transparent wall of the test section parallel, and to emerge parallel. Numerical and experimental interferograms of the flowfields at early stages are shown in **Figure 3** and **4,** respectively. Compared numerical results in **Figure 3** with the corresponding experimental ones in **Figure 4,** it is readily observed that agreement between the numerical and the experimental interferograms is excellent. This indicates that the comparison between numerical and experimental results is easier when two sets of the images are based on the same principle. Under such circumstances, we can reach a conclusion directly and avoid any mis-interpretation of physics.

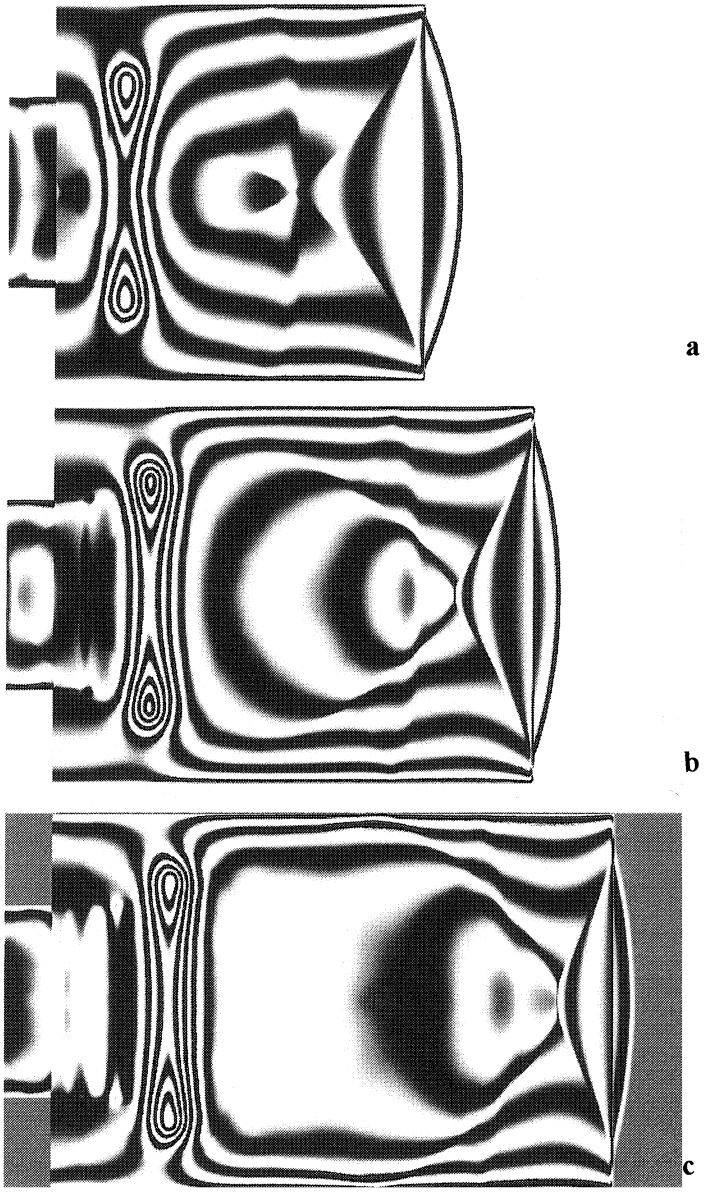

Figure 3. Sequential computational interferograms of the shock wave propagation in a tube with sudden area change in its cross section and the shock wave Mach number is taken as 1.3

4. CONCLUDING REMARCKS

Computational flow visualization based on the common principle of high-speed photography can be used to assist high-speed photography in visualizing shock wave phenomena more clearly and effectively by eliminating background noise in experiments. It also can be used to create a direct comparison between numerical solutions obtained with CFD methods and experimental results. This has proved to be a promising way to approach the reliable validation of numerical solutions, especially for complex flow fields with three-dimensional effects in flow visualization. For such cases, the quantification of experimental interferogram is almost impossible. This kind of the validation with quantitative characters is also an effective approach to the whole flow field validation without any loss of accuracy on both experimental data and numerical results.

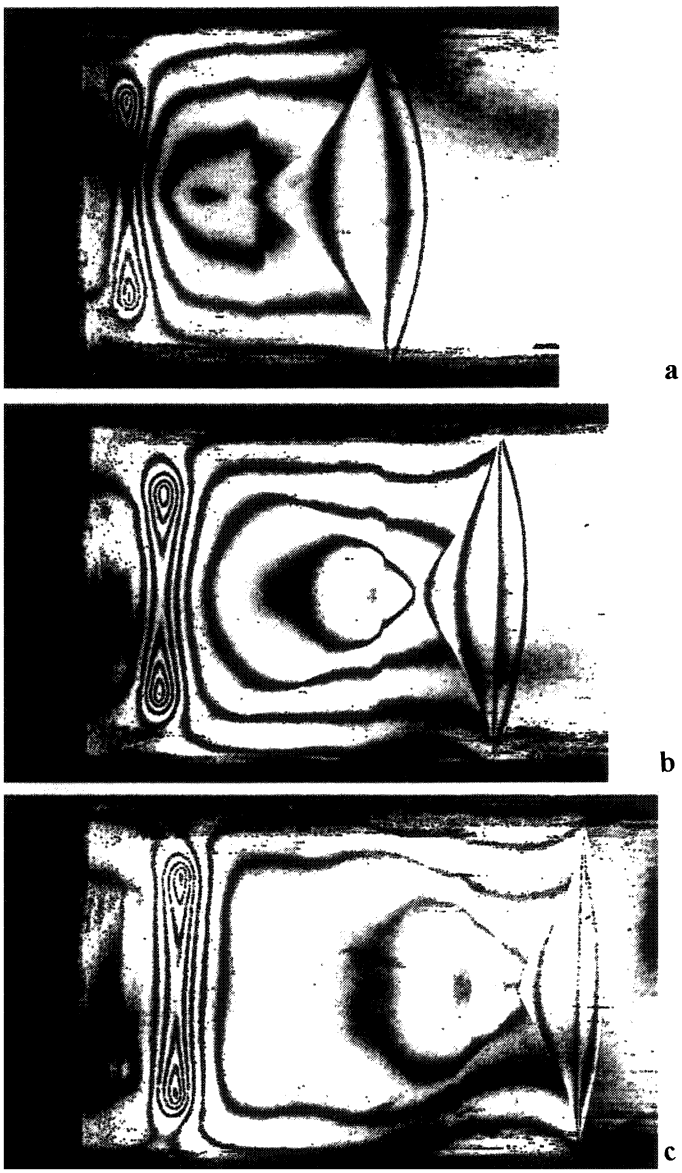

Figure 4. Sequential experimental interferograms of the shock wave propagation in a tube with sudden area change in its cross section and the shock wave Mach number is taken as 1.3

REFERENCES

1. O. Inoue, M. Takahashi and K. Takayama, "Shock wave focusing in a log-spiral dust," *AIAA Journal*, **31**, p.1150, 1993.
2. S.P. Sharma and S. Ruffin, "Density measurements in an expanding flow using holographic interferometry," AIAA Paper 92-0809.
3. A.G. Havener and L.A. Obergefell, "Computational interferometric description of nested flow fields," *Optical Engineering*, **24**, p. 441, 1985.
4. L.A. Yates, " Images constructed from computed flowfields," *AIAA Journal*, **31**, p.1877, 1993.
5. Z. Jiang and K. Takatama, "An investigation into the validation of numerical solutions of complex flowfields," *J. of Comp. Phys*. **151**, p.479-497, 1999.